LBL-26928

Center for Advanced Materials

CAM

Presented at the Fifth International Aluminum-Lithium Conference, Williamsburg, VA, March 27–31, 1989, and to be published in the Proceedings

Influence of Extrinsic Crack Deflection and Delamination Mechanisms on the Cryogenic Toughness of Aluminum-Lithium Alloy 2090: Behavior in Plate (T81) vs. Sheet (T83) Material

K.T. Venkateswara Rao and R.O. Ritchie

February 1989

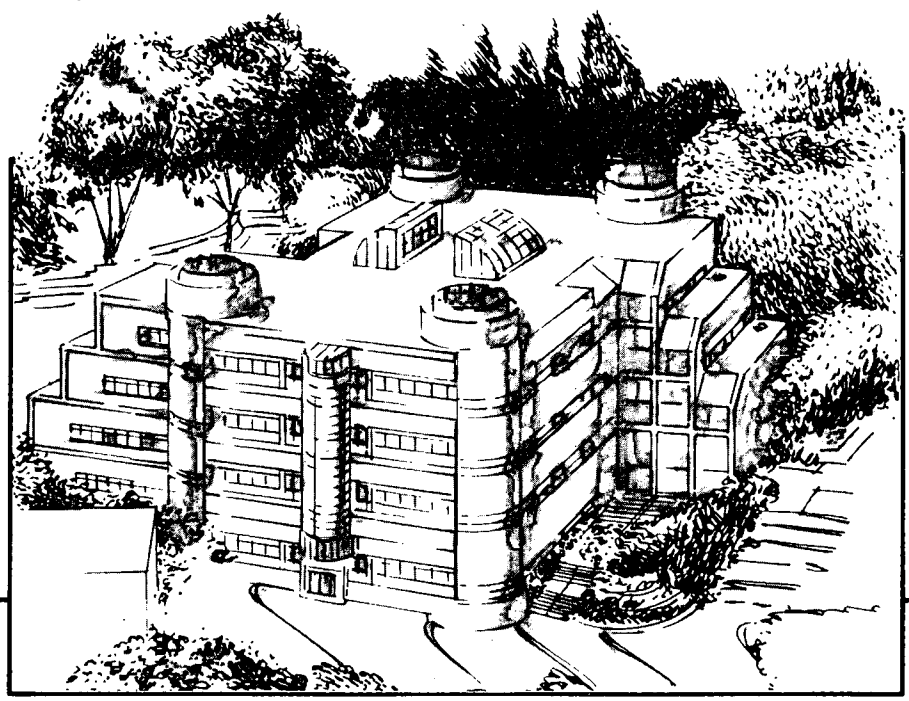

Materials and Chemical Sciences Division

Lawrence Berkeley Laboratory • University of California

ONE CYCLOTRON ROAD, BERKELEY, CA 94720 • (415) 486-4755

Prepared for the U.S. Department of Energy under Contract DE-AC03-76SF00098

DISCLAIMER

LBL-26928

INFLUENCE OF EXTRINSIC CRACK DEFLECTION AND DELAMINATION MECHANISMS ON THE CRYOGENIC TOUGHNESS OF ALUMINUM-LITHIUM ALLOY 2090: BEHAVIOR IN PLATE (T81) VS. SHEET (T83) MATERIAL

K. T. Venkateswara Rao and R. O. Ritchie

Center for Advanced Materials, Lawrence Berkeley Laboratory
and
Department of Materials Science and Mineral Engineering
University of California, Berkeley, CA 94720

February 1989

presented at the Fifth International Conference on Aluminum-Lithium Alloys
Williamsburg, Virginia, March 1989

Work supported by the Director, Office of Energy Research, Office of Basic Energy Sciences, Materials Sciences Division of the U.S. Department Energy under Contract No. DE-AC03-76SF00098.

INFLUENCE OF EXTRINSIC CRACK DEFLECTION AND DELAMINATION MECHANISMS ON THE CRYOGENIC TOUGHNESS OF ALUMINUM-LITHIUM ALLOY 2090: BEHAVIOR IN PLATE (T81) VS. SHEET (T83) MATERIAL

K. T. Venkateswara Rao and R. O. Ritchie*

Cryogenic strength-toughness relationships are examined in 1.6-mm-thick sheet of commercial 2090-T8 aluminum-lithium alloy, and results compared with behavior in 12.7-mm-thick rolled plate. Unlike the significant *increase* in L-T fracture toughness exhibited by thick plate sections at cryogenic temperatures, the thin sheet (of nominally similar composition and microstructure) shows a marked *decrease* in toughness between 298 and 77 K. Such contrasting observations are attributed primarily to the low short-transverse toughness of the 2090-plate material, which results in enhanced through- thickness intergranular splitting during low-temperature fracture and hence to a prominent role of crack-divider delamination toughening.

INTRODUCTION

High-strength aluminum alloys have long been a preferred structural material for many cryogenic applications because of their high strength-to-weight ratio, non-magnetic behavior, stable microstructures and ability to retain strength, ductility and fracture-toughness properties at low temperatures (1). For example, Al-4½wt%Mg (5083-0) and Al-4wt%Cu (2021-T851, 2014-T651) alloys are widely used for liquefied natural-gas tankage and for liquid-hydrogen and liquid-oxygen rocket-propulsion fuel systems; in fact the space shuttle's 8-m-diameter external fuel tanks are fabricated from a heat-treated Al-6wt%Cu 2219-T87 alloy.

Ultra-low density aluminum-lithium alloys have aroused particular interest in recent years for future cryogenic applications (trans-atmospheric and hypersonic vehicles), because of reports (2-8) showing remarkable improvements in their strength-toughness relationships at 77 and 4 K. Specifically, results on commercial Al-Li-Cu-Zr (2090-T81) plate, in the longitudinal and long-transverse (L, T or L-T, T-L) orientations, indicate a 45% increase in strength, 12% increase in elastic modulus and nearly 100% increase in fracture toughness between ambient and liquid-helium (4 K) temperatures. However, it has been subsequently discovered that the enhanced low-temperature toughness is not seen in short-transverse (S-L, S-T) orientations, nor for all aluminum-lithium alloys and aging conditions (4-6)

*Center for Advanced Materials, Lawrence Berkeley Laboratory, and Department of Materials Science and Mineral Engineering, University of California at Berkeley, Berkeley, CA 94720, U.S.A.

Mechanistically, the superior cryogenic toughness of Al-Li alloys has been related to increased homogeneity of plastic deformation from higher strain-hardening rates (7) and strain localization in wider and more closely spaced slip bands (8), and to the solidification of Na, K, and H-rich low melting-point eutectic phases at grain boundaries (3), all mechanisms which fail to explain the concurrent reduction in short-transverse toughness. Alternative explanations (4-6), which account for the toughness variations in all orientations, have focused on the greater tendency at low temperatures for delamination cracking along the weak elongated grain structures perpendicular to the rolling plane (Fig. 1). Akin to laminated composites (Fig. 2), such enhanced short-transverse cracking promotes toughening by crack deflection in the T-S and L-S (crack-arrester) orientations, and toughening by a delamination-induced reduction in through-thickness constraint in the L-T and T-L (crack-divider) orientations (4-6).

As such explanations are still somewhat controversial, the present study is centered on examining the cryogenic toughness and corresponding role of crack-divider delamination toughening in thin sheet of aluminum-lithium alloy 2090-T83, in which through- thickness delamination is not expected to occur; results are compared with those obtained previously (4-7) on 12.7-mm-thick 2090-T81 rolled plate.

EXPERIMENTAL PROCEDURES

Commercial 12.7-mm-thick plate and 1.6-mm-thick sheet of aluminum-lithium alloy 2090 (composition in wt%: Al-2.7%Cu-2.4%Li-0.12%-Zr) were received in the near peak-aged T81 and T83 conditions, respectively. The latter designations refer to proprietary thermo-mechanical treatments for 2090 products, which typically involve homogenization, a water quench, and a 3-6% permanent stretch prior to artificially aging to near peak strength. In the T83 condition, 2090 sheet exhibits in the L-orientation room-temperature yield and ultimate strengths of 505 and 545 MPa, respectively, with an elongation of 6.8%; corresponding strength values for thicker T81 plate are 552 and 589 MPa, with a 9.3% elongation (Table I). However, mechanical properties in both sheet and plate form are strongly anisotropic (9,10).

The grain structure of the plate was unrecrystallized with large pancake-shaped grains, roughly 30 μm thick, 500 μm wide, and elongated several mm in the rolling direction (Fig. 1); fine equiaxed subgrain structures were seen in the thin sheet, indicative of continuous recrystallization within the pancake-shaped grains. Microscopically, both plate and sheet showed evidence of sub-micron intermetallic particles, rich in Cu and Fe and retained during homogenization, distributed as stringers along high-angle grain boundaries. Hardening was achieved by homogeneous matrix distributions of ordered, spherical δ' (Al_3Li) precipitates, Θ'-like (Al_2Cu) and T_1 (Al_2CuLi) platelets, with ß' (Al_3Zr) dispersoids. Limited heterogeneous

precipitation along grain and subgrain boundaries was also evident, resulting in the formation of ~50 and 100 nm wide δ'-precipitate-free zones (PFZs) in the sheet and plate, respectively.

Fracture-toughness tests on the T81 plate were conducted on fatigue-precracked, four-point single-edged-notch bend and double-cantilever beam specimens in the L-T, T-L, L+45°, S-L and S-T orientations; results on the T83 sheet were obtained from resistance-curve (R-curve) measurements on 50-mm-wide compact- tension specimens. Corresponding uniaxial tensile properties were obtained on round and flat tensile specimens (for plate and sheet, respectively) in the longitudinal (L) orientation. Tests were performed at 298 K (room-temperature air), 196 K (CO_2 in ethanol), 77 K (liquid nitrogen), and 4 K (liquid helium). Fracture surfaces and crack-path morphologies were subsequently examined using optical and scanning electron microscopy.

RESULTS

Tensile Properties

The variation in uniaxial tensile properties of sheet and plate 2090 with temperature is listed in Table I. Characteristic of most f.c.c. metals, strength, ductility and strain-hardening exponent for both plate and sheet are increased with decrease in temperature. At 77 K, yield (σ_y) and ultimate strengths are 10 to 40% higher and elongation values up to 75% higher than at room temperature, the magnitude of the effect being somewhat larger in the plate. Tensile failures at low temperatures occurred at maximum load, without evidence of localized necking prior to fracture.

Fracture-Toughness Behavior

Results from plane-strain K_{Ic} and R-curve fracture-toughness tests on plate and sheet 2090-T8 alloys between 298 and 77 K are also listed in Table I; the cryogenic toughness data for the plate are plotted in Fig. 3. As reported previously (4-6), the 2090 plate exhibits a remarkable increase in toughness with decrease in temperature, for specimen orientations in the rolling plane (e.g., L-T, L+45°); short-transverse (S-L,S-T) toughness, which is at least 50% lower than L-T values, conversely shows a small decrease.

TABLE 1 - Fracture-Toughness (L-T) and Tensile (L) Properties of Commercial 2090-T8 Al-Li-Cu-Zr Alloy Sheet and Plate at Various Test Temperatures

Temp. (K)	Yield Strength σ_y (MPa)	UTS (MPa)	% Elong. (on 25 mm)	Work-Hardening Exponent n	Fracture Toughness (MPa$\sqrt{m}$)	Plastic Zone Size* r_y (mm)
1.6-mm-thin sheets						
298	505	549	6.8	0.051	36-43#	0.8
196	531	590	7.1	0.053	35-42	0.7
77	568	674	8.0	0.080	30	0.5
12.7-mm-thick plates						
298	552	589	9.3	0.060	36##	0.7
219	565	614	-	-	38	0.7
77	600	715	13.5	0.150	52	1.2
4+	615	820	17.5	-	65	1.8

* Estimated from $r_y \approx (\frac{1}{2}\pi)(K_c/\sigma_y)^2$.

\# Values correspond to minimum and maximum for plane-stress fracture toughness K_c, measured from R-curves.

##Plane-strain K_{Ic} values

+ After ref. 2.

Such short-transverse fracture surfaces were fully intergranular with little evidence of crack deflection. L-T surfaces in the plate, conversely, had a "plywood-type" appearance, with continuous, intergranular delamination cracks interdispersed between regions of transgranular shear. No apparent differences in fracture-surface morphology were noted between 298 and 77 K, although the incidence and depth of delamination cracks were significantly higher at the lower temperatures (Fig. 4).

Corresponding L-T fracture-toughness behavior and crack-path morphologies at 298 and 77 K for the 2090-T83 sheet are compared in Figs. 5 and 6. In contrast to the 12.7-mm (unrecrystallized) plate, the thin (recrystallized) sheet does not display superior toughness at lower temperatures. At 298 K, toughness increases with crack extension (rising R-curve behavior - Fig. 5) as the spread of plasticity relaxes through-thickness constraint to give a plane-stress (fully 45° slant) fracture (Fig. 6a). Failures at 77 K, on the other hand, appear brittle and in the 1.6-mm-thick sections are mixed mode (slant plus flat), approaching plane-strain conditions. Of particular note is that the crack paths at 77 K show a *reduced* tendency for crack deflection in the loading plane, and moreover show *no evidence* of through-thickness delamination cracking; intergranular-ductile fracture prevails at both 77 and 298 K.

DISCUSSION

It is clear from the present results, and those published elsewhere (2-8,11,12), that the marked increase in toughness of aluminum-lithium alloys at cryogenic temperatures is not a general characteristic of all Al-Li-alloy microstructures, nor of all orientations or product forms. For the current Al-Cu-Li-Zr alloy 2090-T8, although the plane-strain fracture toughness (L-T orientation) in 12.7-mm T81 plate is significantly enhanced at 77 and 4 K compared to ambient temperature, the corresponding "non plane-strain" toughness of 1.6-mm T81 sheet is reduced, despite the fact that the strength, ductility and strain-hardening rates for both plate and sheet are similarly improved. Moreover, as reported previously (4-6), the S-L toughness of the plate also does not show increased toughness at lower temperatures.

Such results negate certain published explanations for the cryogenic toughness behavior of aluminum-lithium alloys, namely that the observed increase in toughness of L-T plate with decrease in temperature is associated with increased homogeneity of slip and a resulting increase in strain-hardening rates (7,8), or with the solidification of grain-boundary liquid phases (3). This follows because both T81 plate and T83 sheet have nominally identical chemical composition, similar aging tempers and hardening precipitates, and display increased strain-hardening coefficients at lower temperatures.

Conversely, explanations based on the notion of crack-divider delamination toughening (4-6) appear to be far more convincing. As described elsewhere (6), the elevation in L-T toughness of the T81 plate with decrease in temperature is attributed to increased through-thickness (short-transverse) splitting perpendicular to the fracture plane at low temperatures (Fig. 4). Such short-transverse splitting, which is associated with a brittle delamination-type intergranular fracture mode, is promoted at low temperatures by the increased yield strength and strain hardening of the alloy (characteristic of stress-controlled fracture (13,14)); it is furthermore consistent with the measured decrease in short-transverse toughness with decreasing temperature. The effect of such splitting is to relieve through-thickness stresses (constraint) in the thick plate; *the fracture mode is then transformed from one of (fully constrained) plane- strain at room temperature to a natural "laminate" of (unconstrained) "near plane-stress" ligaments at lower temperatures*, each with a predominantly slant fracture and a higher toughness than the plane-strain K_{Ic} value. In fact, the spacing of the delaminations is comparable with one to two times the plastic zone size r_y (i.e., comparable with the plane-stress ligament size - Table I, Fig. 4b), and measurements of the fracture toughness with specimen thickness in 2090-T81 correctly predict the low-temperature toughness of the delaminated alloy (6). Moreover, the progressively increasing strength of 2090 with decreasing

temperature further enhances the toughness for this fracture mode, as classical models (15-17) for such (strain-controlled) shear fracture predict that the K_c toughness is proportional to $\sqrt{\sigma_y}$.

In contrast, no such through-thickness splitting is observed in the T83 sheet (Fig. 6), presumably because of the more equiaxed (recrystallized) grain structure and the lack of through-thickness stresses in the thinner section. In this case, *a slant plane-stress fracture at room temperature becomes a mixed plane-stress plus plane-strain (slant plus flat) fracture at low temperatures* (due to diminished crack-tip plasticity), with a consequent decrease on toughness. Note that at both 298 and 77 K, the plastic-zone size r_y is once more comparable with one to two times the thickness of the slant- fracture section - Table I, Fig. 6.

As noted above, such toughening due to short-transverse splitting is also consistent with the high toughness of 2090-T81 in the T-S orientation, as the crack tends to blunt and deflect through ~90° at the short-transverse delaminations (crack-arrester toughening - Fig. 2) (5,6). In fact, the measured T-S toughness is approximately 65 MPa$\sqrt{m}$, which is some four times the short- transverse toughness (6), consistent with recently proposed mechanics criteria for crack deflection at interfaces (18). Moreover, this toughening mechanism has been associated with fracture behavior in laminated steels (19-21), ceramic composites (22) and most recently in high-temperature Al-Fe alloys containing Ce, V and Mo (23), all cases where the inclusion of planes of weakness in the microstructure has resulted in toughened, yet anisotropic, material.

In commercial aluminum-lithium alloys, the weakened short-transverse properties of the plate material result in part from highly elongated and unrecrystallized grain structure which persists after pre-temper stretching, and in part from heterogeneous precipitation along such high-angle grain boundaries and associated solute-denuded, δ'-PFZs. As a result, the Al-Li alloys with best cryogenic toughness are generally the peak- and overaged microstructures. Underaged microstructures, conversely, rarely show evidence of grain-boundary precipitation; the high- angle grain boundaries are thus comparatively stronger, with the result that short-transverse splitting is less apparent and the toughness does not increase markedly at low temperature.

CONCLUSIONS

Based on a study at 298 to 77 K of the temperature dependence of the fracture toughness and uniaxial tensile properties of commercial near peak-aged aluminum-lithium alloy 2090 in 12.7-mm-thick T81 plate and 1.6-mm-thin T83 sheet, the following conclusions may be made:

1. Both plate and sheet of 2090-T8 show increased yield and ultimate tensile strengths, ductility, and strain hardening exponents with decrease in temperature from 298 to 77 K; the magnitude of the improvements is largest in the thick plate.

2. The plane-strain K_{Ic} fracture toughness of the 12.7-mm-thick plate is significantly enhanced in the L-T orientation with decrease in temperature from 298 to 77 K; the corresponding K_c toughness of the 1.6-mm-sheet is significantly decreased. K_{Ic} values for the plate material in the short-transverse (S-L, S-T) orientations are somewhat reduced over the same temperature range.

3. Such observations are attributed primarily to effects of crack-divider delamination toughening. In thick plates containing weak interfaces in a preferred orientation, enhanced splitting along these (short-transverse) interfaces reduces through-thickness constraint at the crack-tip in the divider orientation. Consequently, the plane-strain fracture process is divided into several near plane-stress failures with higher K_c values, thus leading to improvements in toughness at low temperatures. Conversely, in the thin sheet, the lack of through-thickness stresses and the equiaxed recrystallized grain structure act to suppress such splitting; consequently, the toughness of the thin sheet is not enhanced at cryogenic levels, and in fact shows the more commonly expected behavior of progressively lower toughness with decrease in temperature.

ACKNOWLEDGEMENTS

This work was supported by the Director, Office of Basic Energy Sciences, Materials Sciences Division of the U.S. Department of Energy under Contract No. DE-ACO3-76SF00098 through the auspices of the Center for Advanced Materials (Structural Materials Program). Thanks are due to Dr. R. J. Bucci of Alcoa for supplying the alloys and J. E. Miles for experimental assistance.

REFERENCES

(1) Reed, R.P. and Clark, A.F. eds., "Materials at Low Temperatures", ASM International, Metals Park, OH, 1983.

(2) Glazer, J., Verzasconi, S.L., Dalder, E.N.C., Yu, W., Emigh, R.A., Ritchie, R.O. and Morris, J.W., Adv. Cryog. Eng., Vol. 32, 1986, pp. 397-404.

(3) Webster, D., Metall. Trans. A, Vol. 18A, 1987, pp. 2181-93.

(4) Dorward, R.C., Scripta Metall., Vol. 64, 1986, pp. 1379-83.

(5) Venkateswara Rao, K.T., Hayashigatani, H.F., Yu, W. and Ritchie, R.O., Scripta Metall., Vol. 22, 1988, pp. 93-98.

(6) Venkateswara Rao, K.T., Yu, W. and Ritchie, R.O., Metall. Trans. A, Vol. 20A, 1989, in press.

(7) Glazer, J., Verzasconi, S.L., Sawtell, R.R. and Morris, J.W., Metall. Trans. A, Vol. 18A, 1987, pp. 1695-701.

(8) Jata, K.V. and Starke, E.A., Scripta Metall., Vol. 22, 1988, pp. 1553-1556.

(9) Venkateswara Rao, K.T., Yu, W. and Ritchie, R.O., Metall. Trans. A, Vol. 19A, 1988, pp. 549-62.

(10) Bucci, R.J., Mehr, P.L., Sowinski, G., Malcolm, R.C., Kaiser, W.T. and Wygonik, R.H., Alcoa Technical Report No. 57-88-30, Pittsburgh, PA, 1988.

(11) Dew-Hughes, D., Creed, E. and Miller, W.S., Mater. Sci. Technol., Vol. 4, 1988, pp. 106-12.

(12) Yin, Z., Aust, K.T., Weatherly, G.C. and Lloyd, D.J., Can. Metall. Quart., Vol. 26, 1987, pp. 61-69.

(13) Ritchie, R.O., Geneits, L.C.E, and Knott, J.F., in "Microstructure and Design of Alloys", Proc. ICMSA-3, Institute of Metals/Iron and Steel Institute, London, U.K., Vol. 1, 1973, pp. 124-28.

(14) Ritchie, R.O., Knott, J.F. and Rice, J.R., J. Mech. Phys. Solids, Vol. 21, 1973, pp. 395-410.

(15) Mackenzie, A.C., Hancock, J.W. and Brown, D.K., Eng. Fract. Mech., Vol. 9, 1977, p. 167-188.

(16) Ritchie, R.O. and Thompson, A.W., Metall. Trans. A, Vol. 16A, 1985, pp. 233-248.

(17) Knott, J.F., "Fundamentals of Fracture Mechanics", Butterworths, London, U.K., 1976.

(18) Evans, A.G., He, M.Y. and Hutchinson, J.W., University of California at Santa Barbara, CA, Report No. M88-32, 1988.

(19) Embury, J.D., Petch, N.J., Wraith, A.E. and Wright, E.S., Trans. Met. Soc. AIME, Vol. 239, 1967, pp. 114-18.

(20) Leichter, H.L., J. Spacecraft, Vol. 3, 1966, pp. 1113-20.

(21) Ohlson, N.G., Eng. Fract. Mech., Vol. 6, 1974, pp. 459-72.

(22) Evans, A.G. and Marshall, D.B., University of California at Santa Barbara, CA, Report No. M88-29, 1988.

(23) Chan, K.S., Metall. Trans. A, Vol. 20A, 1989, pp. 155-64.

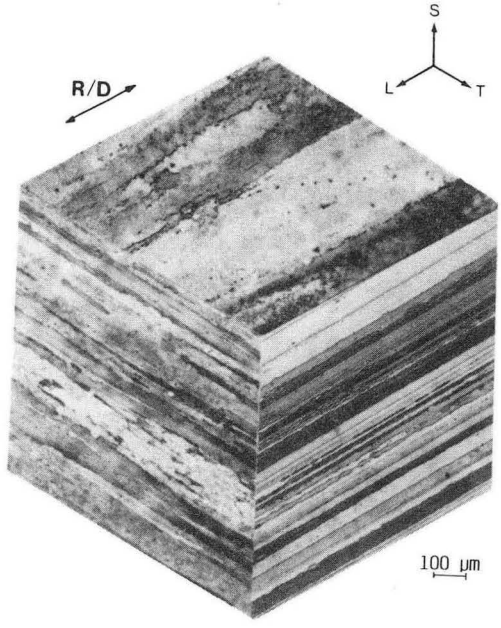

XBB 864-3075A

Figure 1 Three-dimensional optical micrograph of the anisotropic grain structure of commercial rolled 12.7-mm-thick plate of 2090-T81 (Kellers reagent etch).

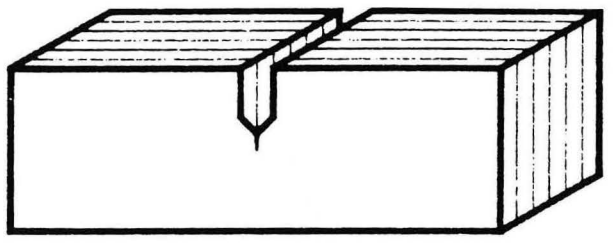

Crack
divider
(L–T,T–L)

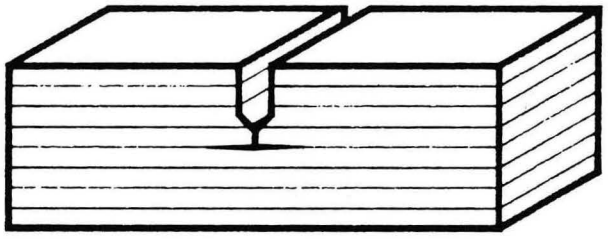

Crack
arrester
(T–S,L–S)

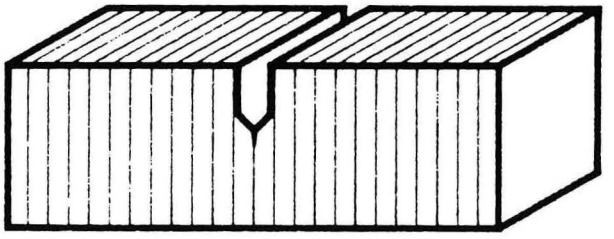

Crack
delamination
(S–L,S–T)

XBL 883-844

Fig. 2: Nomenclature used to describe the various specimen-crack orientations in laminated "composite" materials. Note that T-L and L-T orientations correspond to crack-divider, T-S and L-S to crack-arrester, and S-L and S-T to crack-delamination orientations.

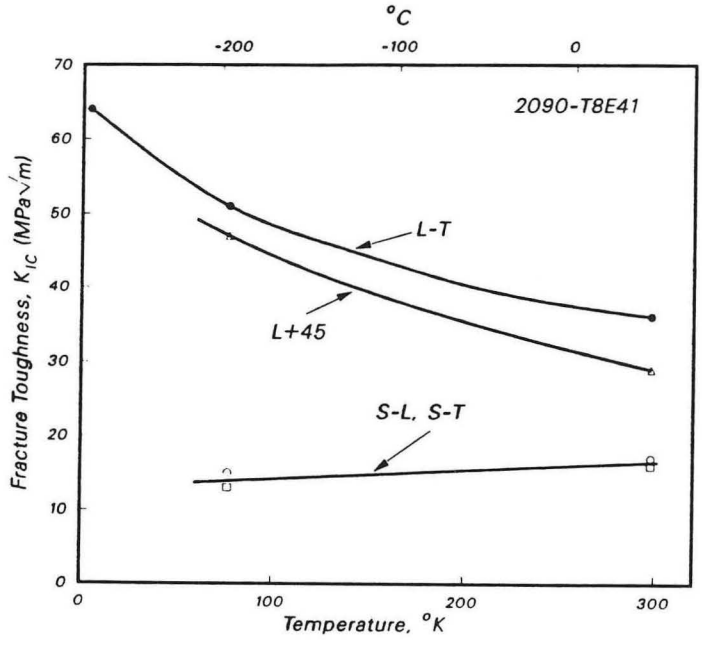

Figure 3 Variation in plane-strain fracture toughness of commercial 2090-T81 alloy plate with test temperature in the L-T, L+45°, S-L and S-T orientations. Improvements in toughness with decreasing temperature are seen for all orientations except the short-transverse (S-L, S-T).

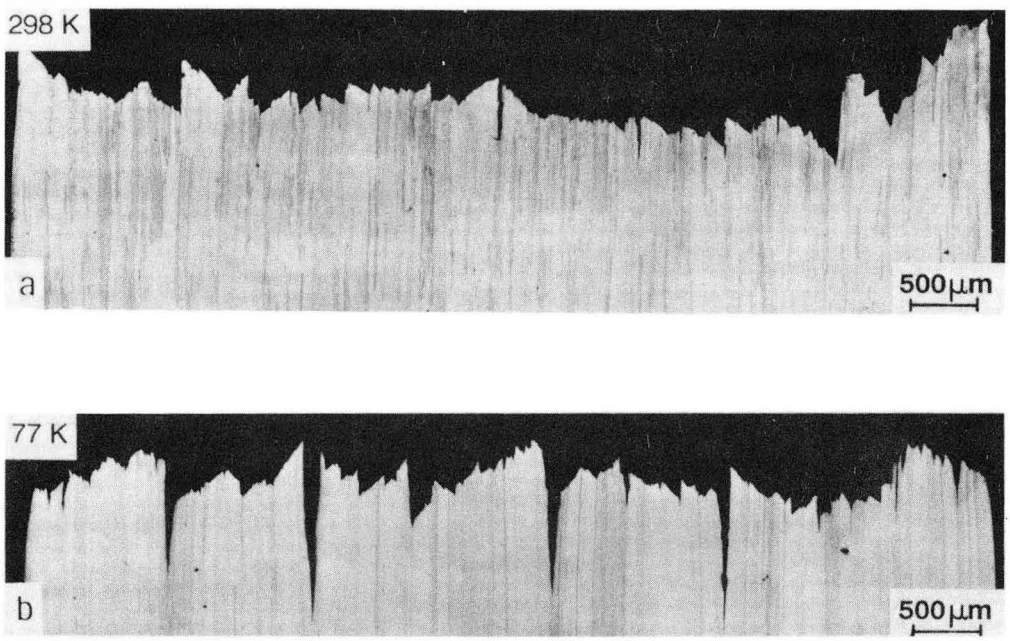

XBB 892-1269

Figure 4 Through-thickness fracture-path morphologies for the 2090-T83 plate at a) ambient (298 K) and b) liquid-nitrogen (77 K) temperatures in the L-T (crack-divider) orientation, showing enhanced delamination at 77 K.

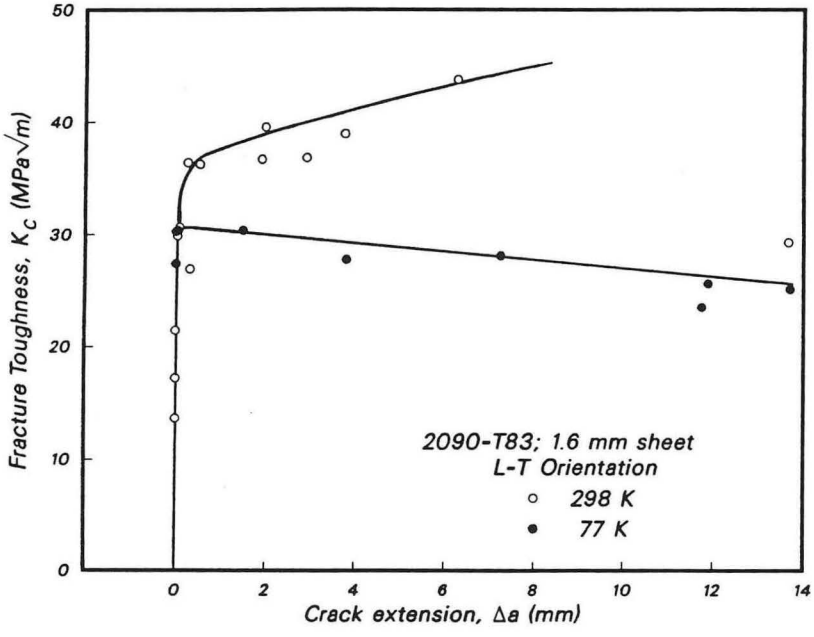

XBL 892-622

Figure 5 Comparison of R-curve behavior in 1.6-mm 2090-T83 sheet at ambient and liquid-nitrogen temperatures. Note that the stress-intensity at crack initiation increases with crack extension at 298 K; behavior at 77 K is typical of mixed plane-stress/strain failures.

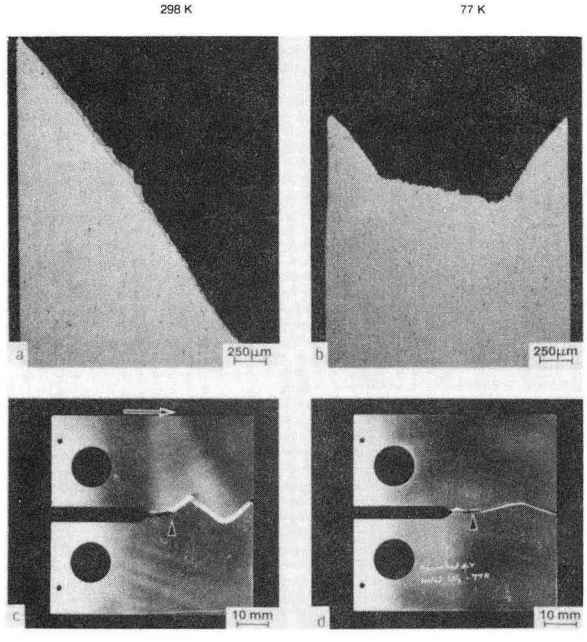

XBB 892-1270

Figure 6 Crack-path morphologies during R-curve testing of 2090-T83 sheet a,c) along the direction of crack growth and b,d) through the thickness of the specimen at room (298 K) and liquid-nitrogen (77 K) temperatures. See text for details.

LAWRENCE BERKELEY LABORATORY
CENTER FOR ADVANCED MATERIALS
1 CYCLOTRON ROAD
BERKELEY, CALIFORNIA 94720